

¹ Vimal Dev Naidu² Mazli B Mustapha³ Syed I.U. Gilani

Performance Evaluation of an Enhanced Solar Still Using Simulink



Abstract: - This study focuses on enhancing the efficiency of solar desalination, particularly for small communities facing water scarcity. Despite the economic viability of solar desalination, the method encounters a technical challenge related to low solar yield. The research proposes innovative solutions, notably the integration of a Compound Parabolic Collector (CPC) and Thermal Energy Storage (TES). The CPC system addresses low solar yield by minimizing losses through reflection, significantly improving the capture efficiency of solar radiation. Additionally, TES serves as a strategic storage component, storing solar energy and providing high energy when needed, thereby enhancing water evaporation rates. Using the SIMULINK platform for evaluation, the study demonstrates that the solar still, enhanced with TES and CPC, consistently produces an average of 15 liters of clean water. This positive outcome underscores the effectiveness of the proposed enhancements and suggests avenues for further refinement. The research not only addresses technical challenges but also establishes a foundation for ongoing improvements in solar desalination technology, offering potential solutions for water-scarce communities.

Keywords: Solar Desalination; Water Scarcity; Compound Parabolic Collector; Solar Still Yield; Sustainable Water Solution; Simulation SIMULINK;

1. INTRODUCTION

Solar desalination stands out as an efficient and practical solution for providing small communities with a sustainable freshwater source. The development of desalination, a crucial solar technology, has effectively addressed the increasing demand for freshwater. Many desalination systems, however, face challenges related to high energy consumption due to capital and energy utilization costs (Akhtar, J). A significant technical issue in solar desalination is the low solar yield, typically producing 4 – 6 L/m².day of fresh water. Research studies propose enhancing the yield by integrating solar stills with thermal backup, indicating the need for improved efficiency (Akhtar, J). Recent global studies suggest that passive solar energy systems could contribute to the sustainability of solar desalination, given their low operating costs. However, existing passive systems exhibit low efficiency. To overcome this, a Compound Parabolic Collector (CPC) with an Evacuated Tube (ET) has been proposed, demonstrating superior performance in recent studies at the Universiti Teknologi PETRONAS, Malaysia. CPCs, proven to be suitable for solar photochemical applications, possess a Reflective surface shaped in an involute pattern surrounding a tube-like cylindrical reactor, providing optimal optics for low solar radiation concentration systems. By incorporating this technology, there is potential to enhance the solar yield through improved integration with solar stills. While solar desalination faces challenges with low solar yield, research studies suggest improvements through the integration of solar stills with thermal backup. Further research is needed to explore thermal backup parameters, including flow rate, heat supply, and the type and size of the thermal back unit, targeting a solar yield of 15-20 L/m².day. This project aims to develop a hybrid seawater desalination technique utilizing solar thermal energy as an external heat source, scaling it to an industrial level through mathematical simulation. MATLAB & SIMULINK software are employed for a detailed mathematical analysis, considering factors like saline water and the glass cover of solar panels, accounting for convection, evaporation, and radiation.

2. SIMULATION PROCEDURE

The simulation was conducted using the MATLAB software, a powerful tool that integrates data analytics and graphics to visualize and explore the environment. Tailored for iterative analysis within design processes, MATLAB employs a programming language specifically designed for expressing matrix and array mathematics. This characteristic allows for efficient and direct handling of mathematical operations, providing a robust platform for parallel computing. In essence, MATLAB facilitates a seamless integration of analytical and graphical

^{1,2,3} Universiti Teknologi PETRONAS, Tronoh, Perak, Malaysia.

1sivan_20002030@utp.edu.my, 2mazli.mustapha@utp.edu.my, 3syedihsham@utp.edu.my

Copyright©JES2024on-line:journal.esrgroups.org

functionalities, making it well-suited for simulations that involve complex mathematical computations and iterative design analyses.

2.1 MECHANISM PRINCIPLE

The assessment of performance validity through numerical simulation will be carried out utilizing the solar still setup established at the solar research site within Universiti Teknologi PETRONAS (UTP). The methodology for evaluation and analysis will encompass mathematical modelling using data gathered from the experimental site. Figure 1 illustrates the fundamental principles of the conceptualized idea.

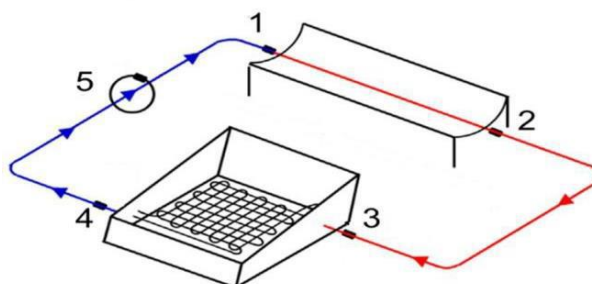


Figure 1. Principle of CPC & TES Solar Still Mechanism

Where:

1. Inlet fluid to CPC, 2. Outlet fluid from CPC, 3. Inlet fluid to the solar still, 4. Outlet fluid from the solar still, 5. Fluid pump.

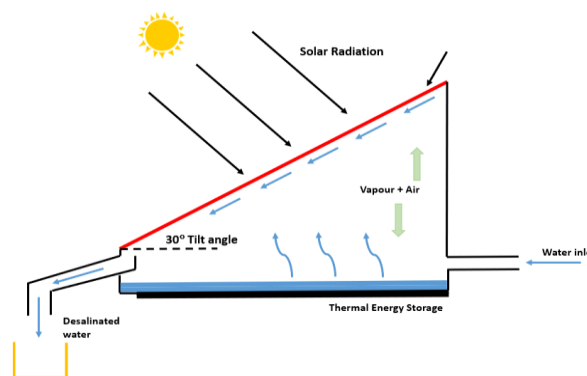


Figure 2. Schematic Diagram of CPC & TES Solar Still

The experimental arrangement, as depicted in Figure 2, is established with reference to various literature studies to set a benchmark. Key components of the solar still include the basin, body (holder), and the glass cover. The optimal strategy involves designing an integrated basin housing the heat exchanger pipe and Thermal Energy Storage (TES), with dimensions set at 1m x 0.6m for length and width, respectively.

The external body is crafted from weather-resistant painted wood. To enhance solar radiation absorptivity in passive operation (**Amer, E.H et al**) (**KositziM et al**) the basin is coated with black paint. The heat exchanger, with high conductivity properties, is fashioned from ½ inch copper pipe, while the body (holder) is constructed from wood. Paraffin wax is chosen as the TES material, validated against literature studies, proving its ability to store more heat in smaller volumes and withstand over 3000 melt-freeze cycles without significant energy storage variation (**C. B. Maia et al**) (**Dai, Y.J.**) (**Gudekar AS et al**) (**Bouronni, K. et al**),

The glass cover, angled at 30° to the horizontal axis (Figure 2), is strategically chosen to optimize the velocity of condensed droplets (**Eslamimanesh, A et al**) (**Enzweilwer RJ et al**). This design prevents droplets from falling directly into the basin, enhancing the efficiency of the evaporation process. The heat exchanger basin is positioned on an insulating layer and wood support, elevated by 1 inch. Experimentally, this study demonstrates that solar yield can be improved while capturing standard solar radiation (**E. N. Baker et al**) (**F.E. Ahmed et al**)

The study and setup, are further substantiated through mathematical modelling simulations in MATLAB to validate the solar still's performance.

2.2 MATHEMATICAL MODELLING

The thermal dynamics and performance of the solar still undergo in-depth evaluation through mathematical models implemented in the MATLAB Simulation software. This model is subjected to rigorous validation and refinement by comparing it with experimental analysis data derived from the setup at UTP Solar Farm. Specifically constructed to assess various operational and design parameters, the model aims to achieve an optimal solar yield. The fundamental operational principle of this design will be optimized to maximize solar absorptivity (**E. N. Baker et al**) (**F.E. Ahmed et al**) (**Farid M.M et al**). The thermodynamic model of the solar still undergoes additional validation and refinement through benchmarking against various studies. Assumptions and variables are carefully constructed to align with the study's output requirements. (**C. B. Maia et al**) (**Dai, Y.J.**) (**Gudekar AS et al**). Several preliminary assumptions are made concerning the working principle of solar desalination, as outlined below:

- i. In this mathematical modelling, it is considered as a one-dimension heat transfer problem where the heat loss on the sidewall will be neglected. [Large surface area compared to the side area].
- ii. In this mathematical modelling, it is considered as a one-dimension heat transfer problem where the heat loss on the sidewall will be neglected. [Large surface area compared to the side area].
- iii. The tilt angle recommended to be in the range of (30° - 40°) for the cover of solar still.

The mathematical model is then constructed based on the energy equation relating to the specification of the model and considering the environmental aspects. The developed model undergoes evaluation incorporating pertinent assumptions, theoretical data from online sources, and experimental data collected during the experimental study. The mathematical model's equations are meticulously examined to understand the impact of each parameter on the performance of the solar still. The primary energy equations considered in this study are: (**Goswami DY et al**) (**Hongfei Zheng**) (**Hou, S et al**).

Convective heat transfer coefficient between water and the glass cover, h_{cwg} . (**Hou, S et al**).

$$h_{cwg} = [0.884 [(T_w - T_g) + [P_w - P_g] (T_w + 273)/(268.9 \times 10^3 P_w)]]^{1/3} \quad (1)$$

Convective heat flux, Q_{cwg} . (**Hongfei Zheng**)

$$Q_{cwg} = h_{cwg} * T_{amb} * (T_w - T_g) \quad (2)$$

Evaporative heat transfer coefficient, h_{ewg} .

$$h_{ewg} = (16.28 \times 10^{-3}) * h_{cw} * (P_w - P_g)/(T_w - T_g) \quad (3)$$

Evaporative heat flux, Q_{ewg} . (**Hou, S et al**).

$$Q_{ewg} = h_{ewg} * T_{amb} * (T_w - T_g) \quad (4)$$

The amount of water condensed in the inner surface of glass cover, kg/s, M_{ewg} . (**E. N. Baker et al**)

$$M_{ewg} = [h_{ewg} A_w (T_w - T_g) * 3600] / h_{fg} \quad (5)$$

Radiation heat transfer coefficient between water and the glass cover, H_{rwg} . (**F.E. Ahmed et al**)

$$h_{rwg} = \epsilon \text{ eff } \sigma [(T_w + 273)^4 - (T_g + 273)^4 - (T_g + 273)^4] / (T_w - T_g) \quad (6)$$

Radiative heat flux, Q_{rwg} . (**Enzweilwer RJ et al**).

$$Q_{rwg} = h_{rwg} * T_{amb} * (T_w - T_g)$$

(7)

Convective heat transfer coefficient between glass cover and the ambient, h_{cga} . (Bouronni, K. et al),

$$h_{cga} = [0.884 [(T_g - T_{amb}) + [P_g - P_{amb}) / (T_g + 273) / (268.9 \times 10^3 P_g)]]^{1/3}] \quad (8)$$

Convective heat flux between glass cover and ambient, Q_{cga} . (Kositzim et al)

$$Q_{cga} = h_{cga} * A_g * (T_g - T_{amb}) \quad (9)$$

Radiative heat transfer between glass cover and ambient, h_{rga} . (Li Puma G et al)

$$T_{sky} = 0.05525 * [(T_{amb} + 273)^{1.5}]$$

$$h_{rga} = 5.67e^8 * [(T_g + 273)^4] (T_{sky} + 273)^4 \quad (10)$$

Convective heat flux between glass cover and ambient, Q_{rga} (M. Drahansky et al)

$$Q_{rga} = h_{rga} * A_g * (T_g - T_{amb}) \quad (11)$$

The numerical model incorporates mathematical Compound Parabolic Collector (CPC) constructions to assess the parametric performance in absorbing solar heat and achieving the highest yield. The energy equations are evaluated and modelled as follows: (Müller-Holst et al)

- i. Assumed radius of the CPC absorber, r.
- ii. Assumed gap between the absorber and the reflectors, lg
- iii. The curvature angle of CPC, Theta A (30°)
- iv. The angle of absorber pipe and the CPC plate

$$Theta M = \text{acos} \left(\frac{r}{r + lg} \right) \quad (12)$$

- v. The distance along the tangential line from the receiver to curve of the CPC, P theta(θ)

$$P \theta (\theta) = (r + lg) * \sin(\theta M) + r * (\theta A - \theta M) \quad (13)$$

The comprehensive energy equation of the CPC is elaborated in detail in the Results & Discussion section, with a detailed expression in MATLAB Simulink.

The validation and simulation in MATLAB rely on input parameters categorized into three subsystems: Operating conditions, Design parameters, and Constant factors. These three subsystems are recognized as the primary factors influencing the performance of the solar still to attain the targeted solar yield in this study. The aforementioned subsystems are further elucidated below (Malato S) (Mistry, K.H) ((Kositzim et al).

Operating conditions are validated in the mathematical model through the consideration of the following parameters: (M. Drahansky et al) (Müller-Holst et al)

- Solar flux, measured in W/m².
- Inlet water temperature.
- Average ambient temperature.
- Average wind speed.
- Inlet feed flow rate.

Design parameters are validated in the mathematical model through the inclusion and consideration of the following factors:

- Glass area, measured in m².
- Basin area, measured in m².
- Still length, measured in meters.
- Still width, measured in meters.
- Transverse distance, measured in meters.
- Longitudinal distance, measured in meters.
- Number of baffles (if included).

Constant factors are validated in the mathematical model through the inclusion and consideration of the following elements:

- Glass Absorptivity.
- Glass Emissivity.
- Glass Transmittance.
- Baffle Absorptivity.
- Water Emissivity.
- Water Absorptivity.
- Heat loss coefficient from the basin and sides, measured in W/m².
- Convection between the basin and saline water, measured in W/m².

In addressing real transient engineering problems, achieving accuracy solely through exact analytical solutions can be challenging. This research adopts a pragmatic approach by establishing a simplified semi-analytical mathematical model. This model combines solutions derived from analytical mathematical methods, empirical correlations gleaned from prior research, and numerical iterations to provide a comprehensive and accurate representation of the transient system under study.

The main assumptions for the simplified semi-analytical mathematical model are outlined as follows (**Nawayseh, N.K et al**) (**Narayan G et al**) (**O. H. Hohmeyer et al**)

- Absorber and PCM are assumed to have uniform temperatures, and temperature gradients within are negligible.
- The thermal capacity and temperature drop of the glazing material are neglected.
- PCM is assumed to undergo isothermal phase change.
- Thermal contact resistance of two components contacting surfaces is neglected.

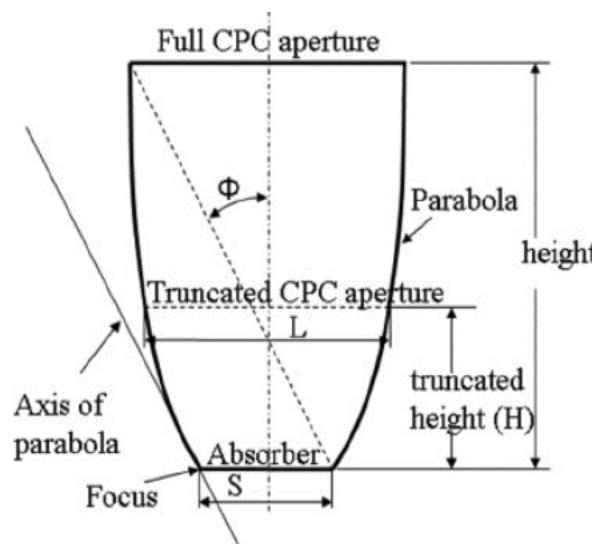


Figure 3. Schematic of Full Height and Truncated height Analysis

Figure 3 shows the interaction of natural convection and surface radiation within two-dimensional parabolic chambers heated from below, with insulated walls and flat top and bottom surfaces. The cavity shape in this numerical analysis is derived from the design of compound parabolic concentrators (CPC) based on non-imaging

optics. To solve the mass, momentum, and energy equations, the study adopts a numerical model based on finite differences. A coordinate transformation is used to transfer the parabolic shape into a rectangular domain, which speeds up the solution procedure. (O. H. Hohmeyer et al) (Rabl A.) (Narayan G et al).

3. RESULT & DISCUSSION

A small fraction of energy is reflected by the water's top surface, and the rest reaches the absorber plate. The maximum energy absorption occurs in the absorber plate, with a portion being reflected. Operating conditions such as solar flux, inlet feed flow rate, solar irradiation, average ambient temperature, and others are validated and evaluated to achieve an optimal solar yield. The energy balance equation makes assumptions such as minimal vapor leakage, little heat loss from the sidewalls of the solar still, and equal temperatures for saline water and the condenser glass cover.

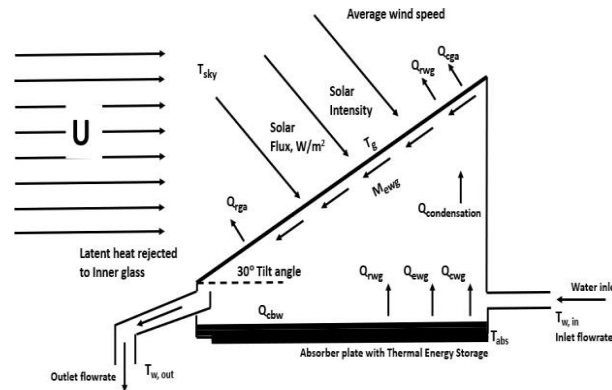


Figure 4. Solar Still Mathematical SIMULINK Model

A small portion of energy is reflected by the top surface of the water, and the remaining energy reaches the absorber plate. The absorber plate absorbs the maximum amount of energy, with a fraction being reflected by it. Operating conditions, including parameters such as solar flux, inlet feed flow rate, solar irradiation, average ambient temperature, etc., are further validated and assessed to optimize the solar yield.

The formulation of energy balance equation is based on the following assumptions:

- No vapor leakage occurs from the solar still.
- Heat loss from the sides of the solar still is negligible
- Saline water and condenser glass cover maintains a uniform temperature.

Figure 4 illustrates the preliminary design simulated in the numerical model evaluation, focusing on the solar still's performance. The energy balance equation, derived as the evaluating parameter throughout the study, forms the basis for this simulation.

The block parameter subsystem, based on the assumptions and energy balance equation, is simulated to generate data across various variable inputs. This mathematical model, derived from the block parameter subsystem, produces a preliminary data chart showcasing the impact of each parameter on the efficient design of the solar still, considering aspects of implementation and commercialization for the market.

Figures 5 and 6 depict the data chart resulting from varying inputs to the solar still performance. This chart is then compared with various trial runs involving different design parameters to evaluate and obtain the most optimal performance. The data chart based on solar flux, solar irradiation, ambient temperature, wind speed, average inlet water temperature, and inlet feed flow rate evaluated between 11:00 am and 4:00 pm. The conditions include an average cloud coverage of 22.3% (according to weather.my), humidity of 84%, wind speed at 3 km/h, and precipitation at 4%.

The comprehensive evaluation of the solar still involves analyzing various parameters, including convective heat flux (Q_{cwg}), evaporative heat flux (Q_{ewg}), the amount of water condensed on the inner surface of the glass cover (H_{rwg}), radiative heat flux (Q_{rwg}), convective heat transfer coefficient between the glass cover and ambient (H_{cga}), convective heat flux between

the glass cover and amb This comprehensive research attempts to comprehend and improve the performance of the solar still system.

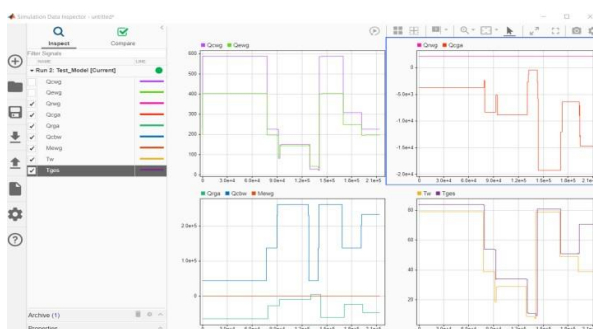


Figure 5. Solar Still SIMULINK Solar Irradiation

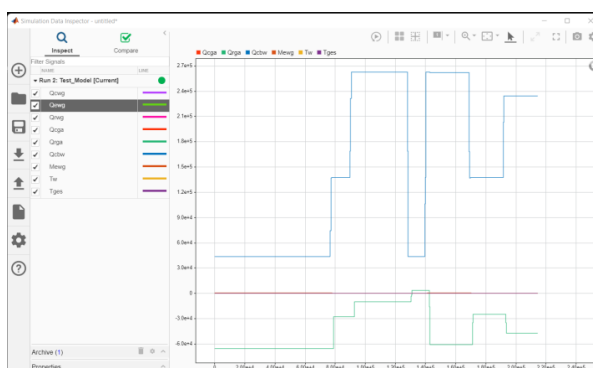


Figure 6. Solar Still SIMULINK Solar Radiation

An explicit energy equation has been derived to align with the designed Compound Parabolic Collector (CPC) and to scrutinize the detailed performance of solar radiation absorption, aiming to maximize the yield in solar desalination. Vital parameters such as the angle of the CPC, radius, and the angle of the absorber tube undergo hypothetical analysis to achieve the highest solar capturing potential. The incident angle of the CPC is assumed to be at least 30 degrees to optimize heat absorption into the water in the absorber tube. The evaluation is based on convective heat flux (Q_{cwg}) and evaporative heat flux (Q_e).

In line with the data collection, on Figure 6, Figure 7 illustrates the thermal absorption evaluated at the full height of the CPC from 11:00 am to 4:00 pm. This evaluation considers an average cloud coverage of 22.3% (according to weather.my), humidity of 84%, wind speed at 3 km/h, and precipitation at 4%. The orange line indicates more than 50% of solar heat being absorbed, the red-coloured line indicates less than 70% of total heat, and the blue-coloured line indicates more than 30% of solar heat being absorbed.

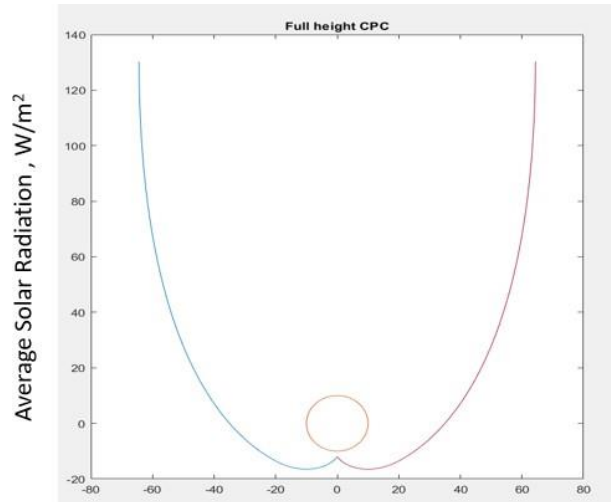


Figure 7. SIMULINK Full Height CPC Model Heat Graph

Figure 8 depicts the thermal absorption for a truncated Compound Parabolic Collector (CPC) under the same parameters as illustrated in Figure 7. The analysis concludes that thermal absorption varies significantly in relation to the height, radius, and area of the design. The orange line indicates more than 50% of solar heat being absorbed, the red-coloured line indicates less than 70% of total heat, and the purple-coloured line indicates more than 90% of solar heat being absorbed.

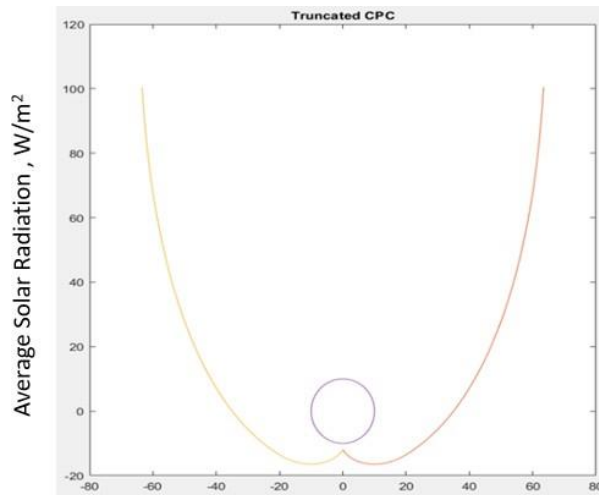


Figure 8. SIMULINK Truncated CPC Model Heat Graph

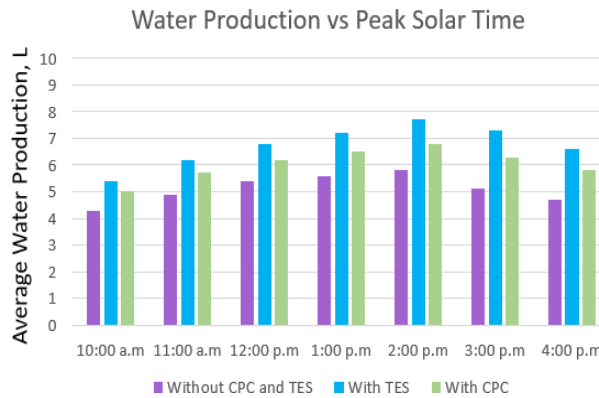


Figure 9. Average Clean Water Production Comparison without TES and with CPC & TES

The data obtained from the analysis of solar absorption in Figure 7 and Figure 8 is integrated into the SIMULINK model to assess the impact of solar absorption on clean water production. Figure 9 presents a comparison of data on clean water production without Compound Parabolic Collector (CPC) and Thermal Energy Storage (TES), with only TES, and with only CPC. The benchmark for this data is derived from a typical solar still, which produces an average of 4-6 liters of clean water. In contrast, the clean water production with only CPC and only TES shows an average of 6-9 liters.

The analysis indicates that the incorporation of both Compound Parabolic Collector (CPC) and Thermal Energy Storage (TES) in a single system significantly enhances the production of clean water through solar still technology, with minimal energy losses. This conclusion is drawn from the data evaluation conducted between 11:00 am and 4:00 pm, accounting for an average cloud coverage of 22.3% (according to weather.my), humidity of 84%, wind speed at 3 km/h, and precipitation at 4%.

Nonetheless, further scrutiny and evaluation of the data and conclusions derived from data study are deemed necessary to ensure that the amount of solar energy captured and stored is notably high compared to the initial data assessment (Figure 10). Therefore, the MATLAB SIMULINK analysis will provide additional insights into the evidence of minimal solar losses to the environment, potentially leading to a significant increase in clean water production.

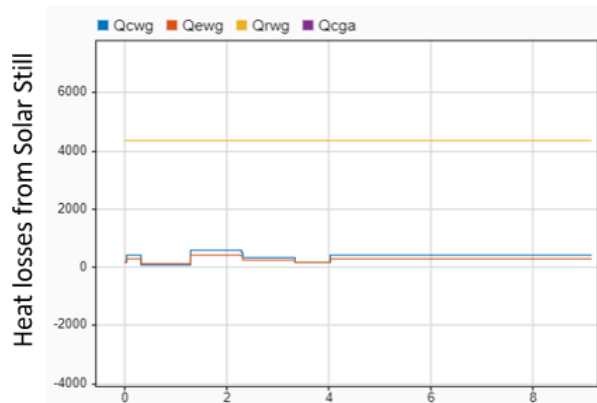


Figure 10. SIMULINK MATLAB Solar Absorption Analysis $\Delta T = 2$

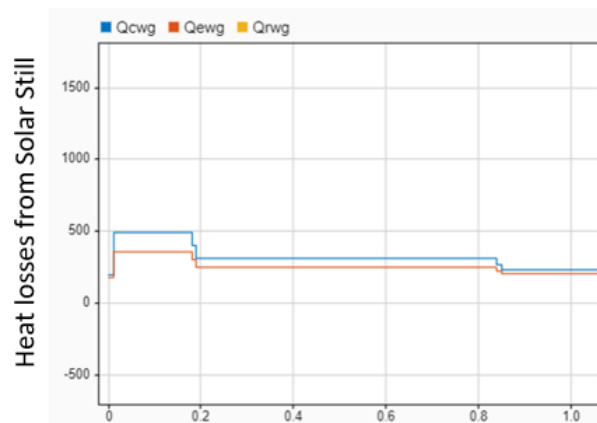


Figure 11. SIMULINK MATLAB Solar Absorption Analysis with $\Delta T = 0.2$

Figure 10 and 11 illustrate the numerical evaluation conducted to study the amount of solar energy captured and stored concurrently with the amount of energy lost during the operation of the solar still. In these figures, Q_{cwg} represents the convective heat flux, Q_{ewg} represents the evaporative heat flux, and Q_{rwg} represents the radiative heat flux.

The distinction between Figure 10 and 11 lies in the precision of data analysis of energy losses. In Figure 10, the time difference taken into consideration is $\Delta T = 2$, whereas in Figure 11, the time difference taken into

consideration is $\Delta T = 0.2$. This is done to study and evaluate the precise energy loss from the Compound Parabolic Collector (CPC).

It is concluded that there is minimal heat loss upon the addition and incorporation of CPC and Thermal Energy Storage (TES). The enhancements in terms of design parameters carried out in the Figure 6, 7, and 8 demonstrated significant results in improving the solar still performance, leading to increased solar yield. The minimal energy loss and high solar capturing through an angular CPC and the addition of TES in solar still technology prove the technology is highly viable for clean water production.

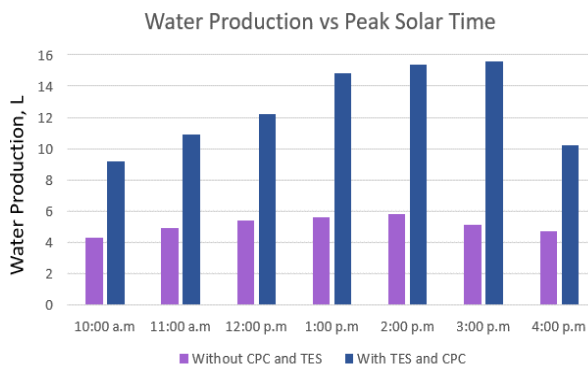


Figure 12. Average Clean Water Production with TES and CPC

The data collected from the study in Figure 10, and figure 11 are fed into the SIMULINK analysis to study the effect of enhancements on clean water production. The data interprets that the amount of clean water production reached an average high of 15.8 L and an average low of 9.2 L. The incorporation of CPC and TES has shown a drastic increase in solar capturing, energy storage, and, importantly, the production of clean water increases from an average of 4-6 L (based on common solar still) to an average of 14 L (with the addition of CPC and TES).

For further validation of the effect of CPC and TES, cumulative data has been collected to simulate the comparison of enhancement for the months of February and March. Below is the tabulated data showing the comparison made for these months.

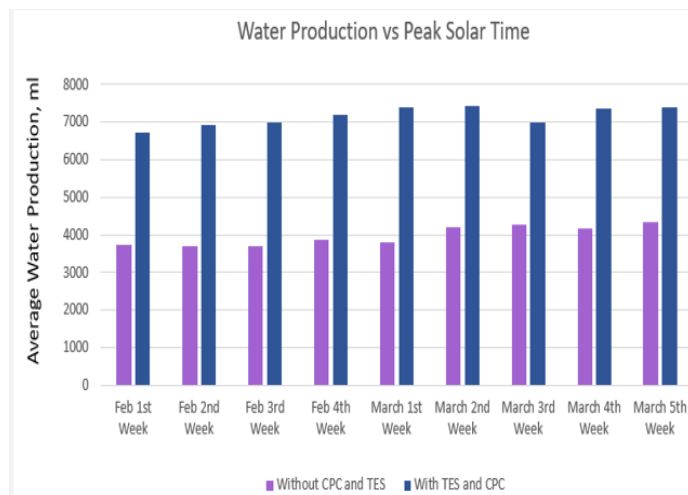


Figure 13. Average Clean Water Production with TES and CPC for the month of February - March.

The data in Figure 13 interprets that the amount of clean water production via CPC and TES reached an average high of 7.3 L and an average low of 6.7 L, compared to without CPC and TES, which had an average high of 4.2 L and an average low of 3.8 L.

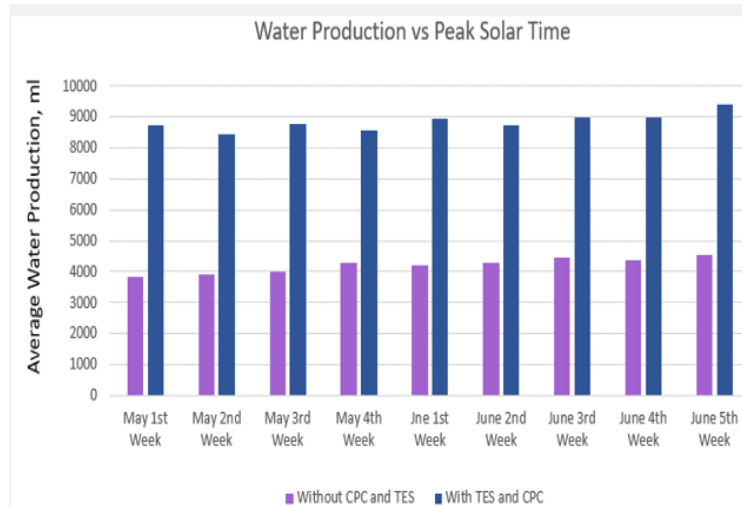


Figure 14. Average Clean Water Production with TES and CPC for the month of May- June

The data in Figure 14 validates that the amount of clean water production via CPC and TES reached an average high of 9.3 L and an average low of 8.4 L, compared to without CPC and TES, which had an average high of 4.43 L and an average low of 3.9 L.

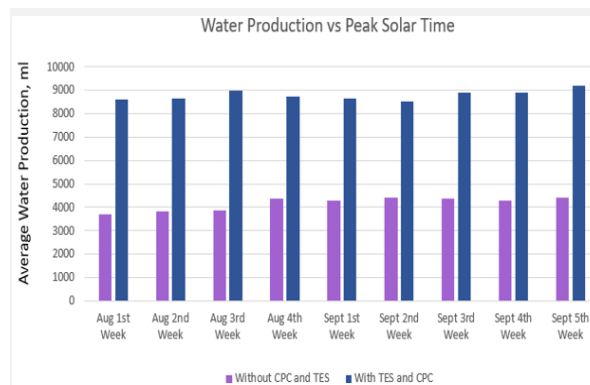


Figure 15. Average Clean Water Production with TES and CPC for the month of August - September.

The data in Figure 15 illustrates that the amount of clean water production via CPC and TES reached an average high of 9.1 L and an average low of 8.6 L, compared to without CPC and TES, which had an average high of 4.3 L and an average low of 3.8 L.

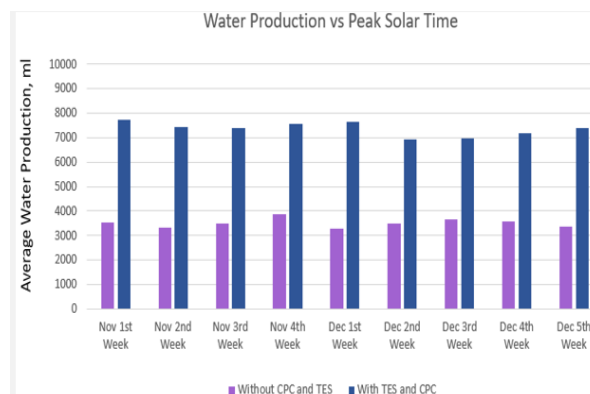


Figure 16. Average Clean Water Production with TES and CPC for the month of November - December.

The chart in Figure 16 visualizes that the amount of clean water production via CPC and TES reached an average high of 7.9 L and an average low of 7 L, compared to without CPC and TES, which had an average high of 3.9 L and an average low of 3.2 L.

On a typical sunny day, solar panels maximize their yield by harnessing abundant sunlight for electricity generation. However, on a cloudy day, solar yield significantly decreases due to reduced sunlight, resulting in lower energy output from the panels. To further validate these conditions, average data has been collected and evaluated using the Simulink software developed in this study. The interpretation of the data is visualized in Figure 17.

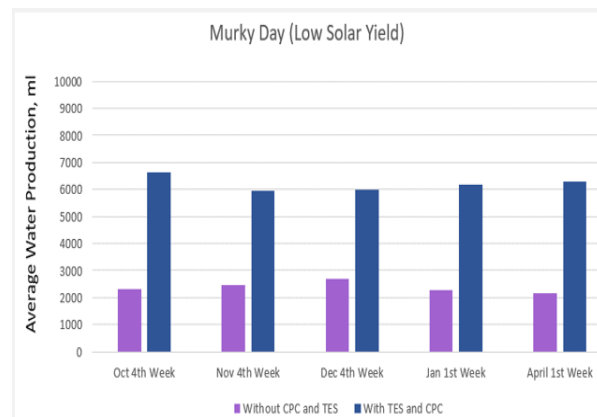


Figure 17. Average Clean Water Production with TES and CPC during murky day.

Incorporating Thermal Energy Storage (TES) and Compound Parabolic Concentrators (CPC) into the solar still significantly boosts clean water production, highlighting the substantial improvement that CPC and TES bring to the system's efficiency, especially during overcast days. This synergistic approach not only enhances water yield but also underscores the potential for sustainable and efficient desalination solutions in regions with abundant sunlight. The data in Figure 24 illustrates that the amount of clean water production during cloudy days via CPC and TES reached an average high of 6.6 L and an average low of 5.9 L, compared to without CPC and TES, which had an average high of 2.9 L and an average low of 2.2 L.

4. CONCLUSION

In conclusion, the integration of Thermal Energy Storage (TES) and Compound Parabolic Concentrators (CPC) into the solar still system has yielded compelling results, significantly elevating clean water production levels. Through meticulous experimentation and analysis, our research demonstrates that CPC and TES technologies synergistically enhance clean water production, offering a promising avenue for the advancement of sustainable and efficient desalination solutions, even during adverse weather conditions. These findings underscore the potential of CPC and TES as critical components in the quest for reliable and environmentally friendly freshwater generation. Further exploration and optimization of these technologies hold great promise for addressing global water scarcity challenges and ensuring a more resilient and sustainable water supply. The data above strengthen the validation of CPC and TES to increase the yield performance as targeted in the research objectives.

Acknowledgement: I would like to extend my sincere appreciation to Universiti Teknologi PETRONAS and Professor Dr Syed Ihtsham ul Haq Gilani for providing invaluable support during my research and contributing to the successful completion of this paper.

References:

1. Akhtar, J. (2019). "Investigation of gap losses in a modified compound parabolic concentrating collector with evacuated tube receiver" IOP Conference Series: Materials Science and Engineering, 863(1).
2. Amer, E.H., Kotb, H., Mostafa, G.H. and El-Ghalban, A.R. (2009) Theoretical and Experimental Investigation of Humidification-Dehumidification Desalination Unit. *Desalination*, 249, 949-959.
3. Bouronni, K., Chaibi, M.T. and Tadrist, L. (2001). Water Desalination by Humidification and Dehumidification of Air: State of the Art. *Desalination*, 137, 167-176.
4. C. B. Maia, F. V. M. Silva, V. L. C. Oliveira, and L. L. Kazmerski (2019). "An overview of the use of solar chimneys for desalination," *Sol. Energy*, vol. 183, no. December 2018, pp. 83– 95.
5. Dai, Y.J., Wang, R.Z. and Zhang, H.F. (2002). Parametric Analysis to Improve the Performance of a Solar Desalination Unit with Humidification and Dehumidification. *Desalination*, 142, 107-118.
6. Eslamimanesh, A. and Hatamipour, M.S. (2010). Economical Study of a Small-Scale Direct Contact Humidification-Dehumidification Desalination Plant. *Desalination*, 250, 203-207.

7. Enzweilwer RJ, Mowery DL, Wagg LM, Dong JJ (1994). A pilot scale investigation of photocatalytic detoxification of BETX water. In: Proceedings of ASME international solar energy conference. San Francisco, USA; p.155–61.
8. E. N. Baker (2017), "science," IUCrJ, vol. 4, no. 1, pp. 1–2.
9. F. E. Ahmed, R. Hashaikeh, and N. Hilal (2019). "Solar-powered desalination – Technology, energy and future outlook," *Desalination*, vol. 453, no. October 2018, pp. 54–76.
10. F. Ahmed, Siwar Chamhuri & Rawshan Ara Begum (2014). "Water resources in Malaysia: Issues and challenges", *Journal of Food Agriculture and Environment* 12(2):1100-1104.
11. Farid, M.M., Parekh, S., Selman, J.R. and Al-Hallaj, S. (2003). Solar Desalination with a Humidification-Dehumidification Cycle: Mathematical Modeling of the Unit. *Desalination*, 151, 153-164.
12. Gudekar AS, Jadhav AS, Panse SV, Joshi JB, Pandit AB (2013). Cost effective design of compound parabolic collector for steam generation. *Solar Energy* 2013;90: 43–50.
13. Goswami DY, Sharma SK, Mathur GD, Jotshi CK (1997). Analysis of solar detoxification systems. *Solar Energy Engineering* 1997;119:108.
14. Hongfei Zheng (2017). "Solar Energy Desalination Technology", published by Elsevier, UK.
15. Hou, S. and Zhang, H. (2008). A Hybrid Solar Desalination Process of the Multi-Effect Humidification Dehumidification and Basin-Type Unit. *Desalination*, 220, 552-557.
16. Kositzim, PoulivosI, MalatoS (2014). Solar photocatalytic treatment of synthetic municipal waste water *Research*, 38:1147–54.
17. Li Puma G, Brucato A. (2017). Dimensionless analysis of slurry photocatalytic reactors using two-flux and six-flux radiation absorption-scattering models. *Catalysis Today*.122:78–9.
18. M. Drahansky et al. (2016). "We are IntechOpen, the world's leading publisher of Open Access books Built by scientists, for scientists TOP 1 %," *Intech*, vol. i, no. tourism, p. 13.
19. Müller-Holst, H., Engelhardt, M., and Scholkort, W. (1999) Small-Scale Thermal Seawater Desalination Simulation and Optimization of System Design. *Desalination*, 122, 255-262.
20. Malato S, BlancoJ, Alarcon CD, Maldonado MI, Fernandez-IbanezP (2017). Photocatalytic decontamination and disinfection of water with solar collectors. *Catalysis Today*, 122:137–49.
21. Mistry, K.H., Mitsos, A.H. and Lienhard V, J.H. (2011). Optimal Operating Conditions and Configurations for Humidification-Dehumidification Cycles. *International Journal of Thermal Sciences*, 50, 779-789.
22. Nawayseh, N.K., Farid, M.M. Omar, A.A., Al-Hallaj, S. and Tamimi, A.R. (1997). A Simulation Study to Improve the Performance of a Solar Humidification-Dehumidification Desalination Unit Constructed in Jordan. *Desalination*, 109, 277-284.
23. Narayan, G., Sharqawy, M.H., Lienhard V, J.H. and Zubair, S.M. (2010). Thermodynamic Analysis of Humidification Dehumidification Desalination Cycles. *Desalination and Water Treatment*, 16, 339-353.
24. O. H. Hohmeyer and S. Bohm, "Trends toward 100% renewable electricity supply in Germany and Europe: A paradigm shift in energy policies," *Wiley Interdiscip. Rev. Energy Environ.*, vol. 4, no. 1, pp. 74–97, 2015.
25. Rabl A, Goodman NB, Winston R. (1979). Practical design considerations for CPC solar collectors. *Solar Energy*. 22:373–81.